Developmental Cell, Volume *58*

Supplemental information

A small noncoding RNA links ribosome recovery and translation control to dedifferentiation during salamander limb regeneration

Elaiyaraja Subramanian, Ahmed Elewa, Gonçalo Brito, Anoop Kumar, Åsa Segerstolpe, Christos Karampelias, Åsa Björklund, Rickard Sandberg, Karen Echeverri, Weng-Onn Lui, Olov Andersson, and András Simon

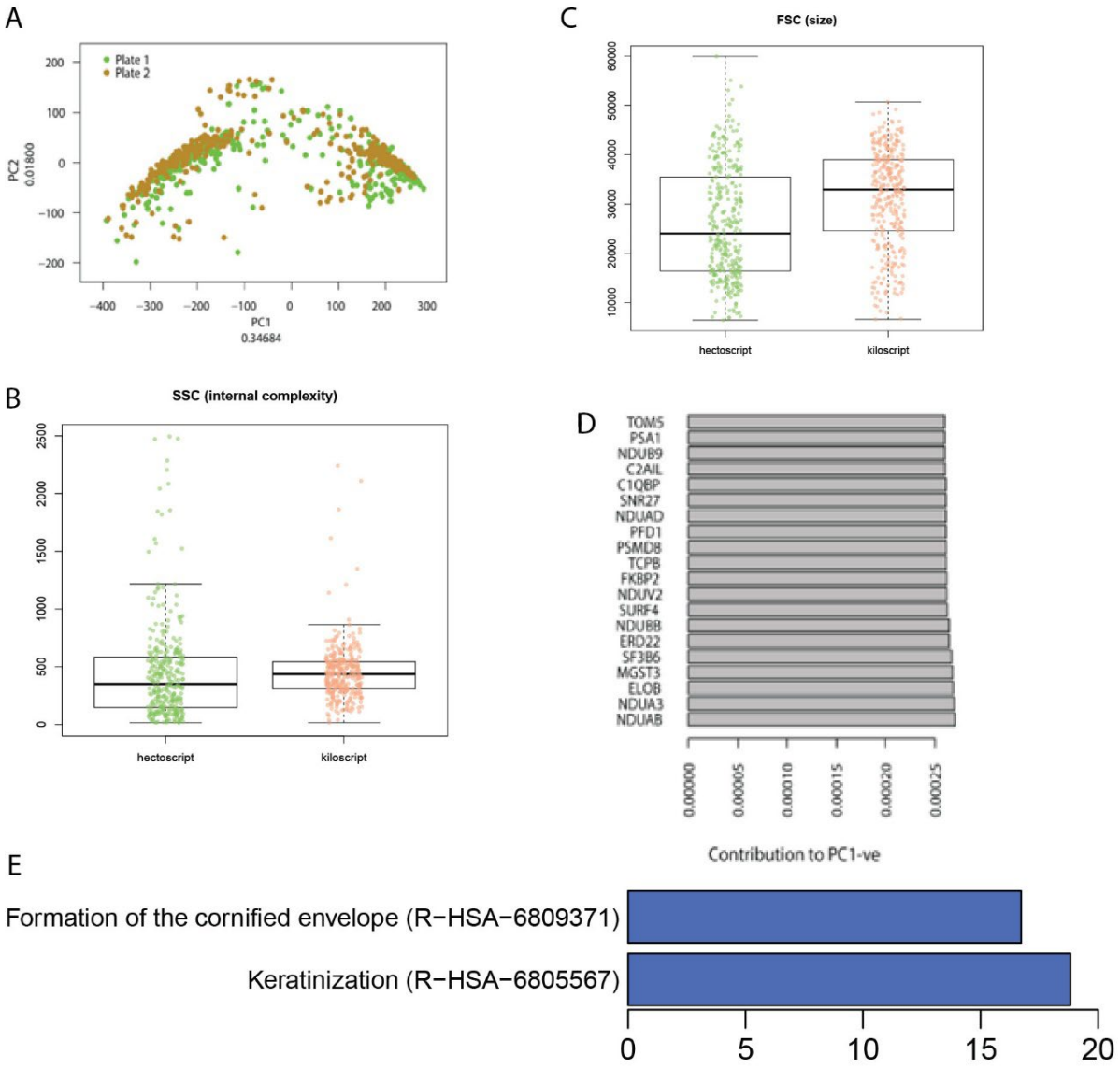

Figure S1. Single-cell RNAseq of the blastema from the adult newt, *Notophthalmus viridescens*, Related to Figure 1. (A) A principal component analysis with cells labeled according to their plate (batch) for visual inspection and exclusion artefacts resulting from batch effect. (B) Boxplot of side scattering (SSC) which is a FACS parameter indicative of internal complexity. No significant difference between Hectoscript and Kiloscript cells observed (Welch Two Sample t-test, mean = 449 vs 451, t = 0.091246, df = 533.37, p-value = 0.9273). (C) Boxplot of forward scattering (FSC) which is a FACS parameter indicative of cell size. A significant difference exists between cell sizes of Hectoscript and Kiloscript cells (Welch Two Sample t-test, mean = 25899 vs 31176, t = 6.4047, df = 656.11, p-value = 2.874e-10). (D) Top contributors to the negative axis of principal component 1 and thereby distinguishing features of Kiloscript cells. (E) Hectoscript cells show an enrichment of genes related to cell keratinization and formation of the cornified envelope (two related processes) using Reactome Pathway Enrichment analysis.

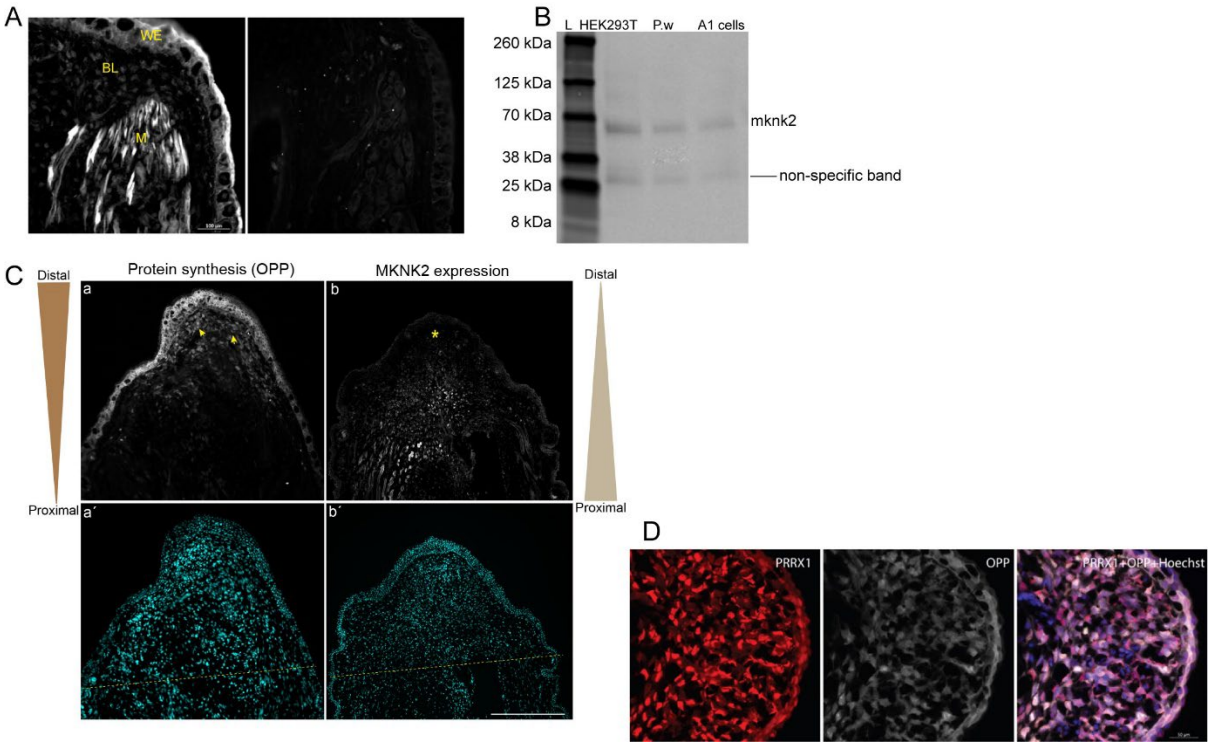

Figure S2. **Expression of MKNK2 during regeneration, Related to Figure 2.** (**A**) MKNK2 antibody shows high reactivity in the muscle fibers adjacent to the amputation plane of the *P. waltl* larval limb blastema (left panel). Right panel shows reactivity with a non-specific Rabbit anti-RFP antibody at matched concentration as a control. The sections represent longitudinal plane. WE, wound epithelium; BL, blastema; M, muscle. Scale bar, 100 µm. (**B**) An immunoblot showing reactivity of rabbit MKNK2 antibody against lysates from HEK293T cells, newt limb tissues and cultured newt A1 cells. (**C**) Reverse correlation between MKNK2 expression and protein synthesis in a limb blastema. (a) Nascent protein synthesis levels in a limb blastema of larval newt *P. waltl*. The arrows point to distal tip cells with moderate to high protein synthesis. Note the substantial reduction in protein synthesis levels in the proximal limb regenerate. (b) A mid-bud stage limb blastema showing reactivity with an antibody to MKNK2. Note the low MKNK2 levels in the distal tip (asterisk). The images are representative longitudinal sections and not from a matched pair. All the limb blastemas we analyzed have shown a similar trend both in MKNK2 expression and OPP uptake (n=5). In lower panels the dotted line indicates plane of limb amputation (a', b'). The sections are stained with a nuclear dye Hoechst 33258. Scale bar, 500 µm. (**D**) A representative image from a cercosporamide-treated limb blastema from larval newt (*P. waltl*) shows PRRX1-positive cells and uptake of OPP by these cells. Scale bar, 50 µm.

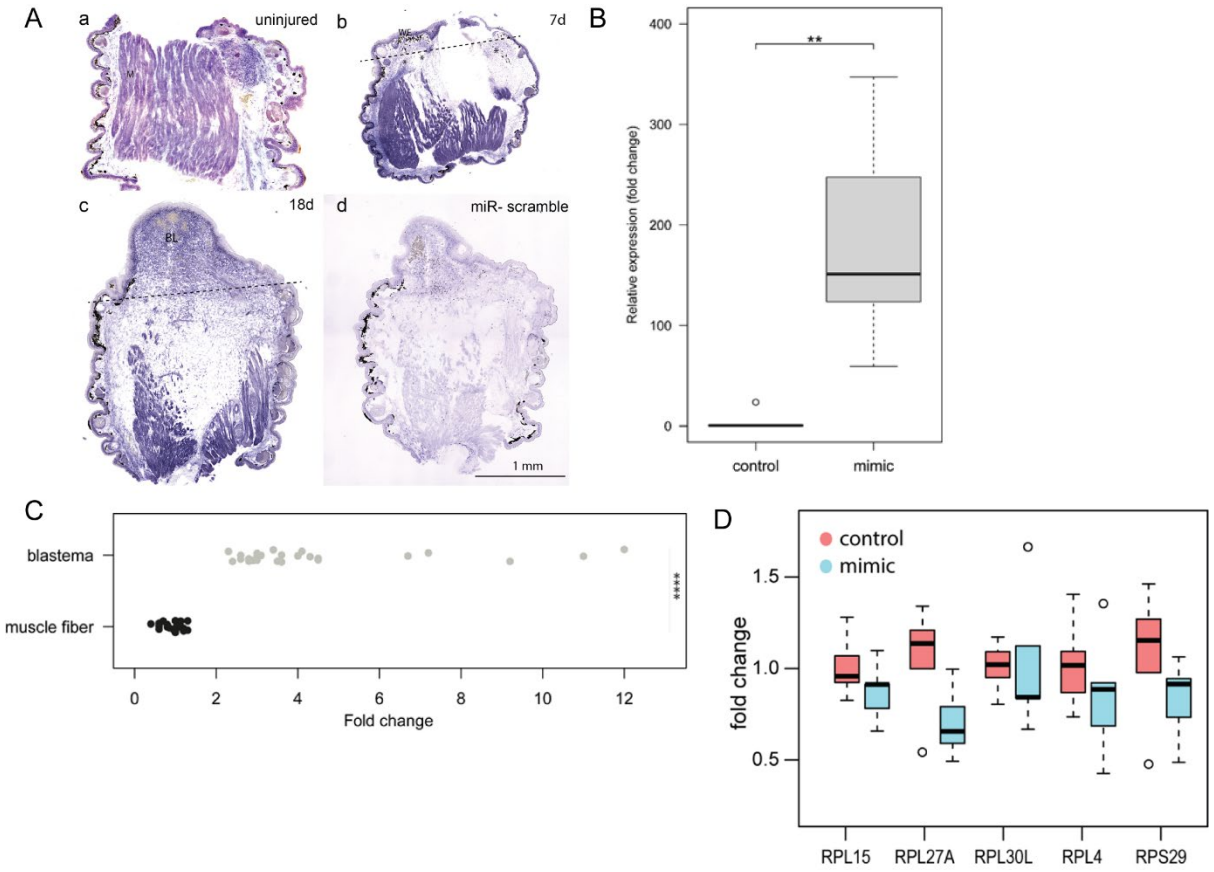

Figure S3. miR-10b expression and regulation of ribogenes, Related to Figure 3. (**A**) In situ hybridization with a miR-10b probe shows reactivity of the limb regenerate at various stages of regeneration in the adult newt *P. waltl*. (a) A section through an uninjured proximal limb. Note the high activity of miR-10b in muscle tissues. (b) 7d limb regenerate. The areas underneath the wound epithelium (asterisks) show relatively low expression compared to the uninjured proximal muscle bundles. (c) The blastema cells show moderate level of miR-10b expression throughout the accumulated cells. However, it is lower than the uninjured stump muscle. (d) The limb tissues show no specific reactivity to a scramble microRNA probe as a control. All sections were cut in longitudinal plane. The dotted line indicates the level of amputation. BL, blastema; M, muscle; WE, wound epithelium. Scale bar = 1 mm. (**B**) Expression of miR-10b in limb blastema after injection of a synthetic mimic. The tissues were collected and analyzed for miR-10b expression by qRT-PCR 3d after electroporation of miR-10b mimic into the larval newt, *P. waltl*. Contralateral control blastema was injected with non-specific miRNA as control. Welch's t-test, **P< 0.01 (n = 6). (**C**) Comparison of ribogene expression in blastema cells and muscle fibers. The muscle tissues were dissected out from larval newts (*P. waltl*) and cleared of non-muscle components before processing. The limb blastema along with the muscle tissues were processed and analyzed by qRT-PCR (n=5). Welch Two Sample t-test t = -6.5851, df = 24.381, ****P< 0.0001). (**D**) Ribogene expression after increasing miR-10b levels in limb blastema by a synthetic mimic. Ribogene levels were evaluated 3d after mimic injection into the larval limb blastema by qRT-PCR. (n = 5 per group).

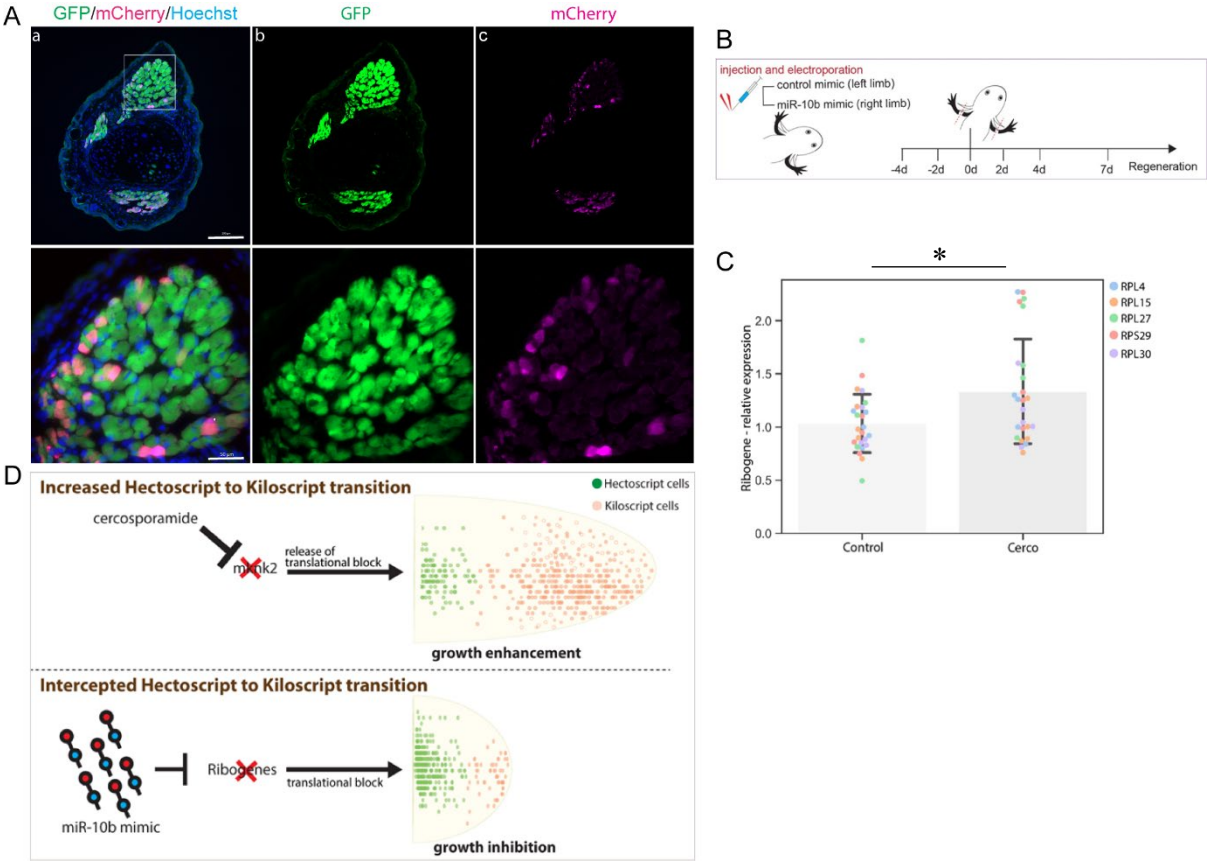

Figure S4. Perturbation of miR-10b during regeneration, Related to Figure 4. (**A**) Induction of Cre by electroporation in transgenic larval newts tgSceI(*CAG-loxP-GFP-loxP-mCherry*)[Simon] leads to activation of mCherry in muscle bundles (a-c; cross sections of forelimb). Lower panel is a magnified area of the inset in (a). The Respective channels are split to show the Cre-induced conversion of muscle fibers from GFP to mCherry. Scale bars, upper panel (200 µM); lower panel (50 µm). (**B**) Illustration of miR-10b mimic overexpression experiment in larval *P. waltl*. miR-10b mimic or control mimic were injected and focally electroporated into the upper forelimb area. (**C**) Ribogene expression in cercosporamide-treated limb blastema. Early larval limb blastema of *P. waltl* were treated with 1 µM cercosporamide or DMSO-control for 24h. The tissue samples were collected and ribogenes (RPL4, RPL15, RPL27, RPS29 and RPL30) were analyzed by qRT-PCR. Cumulative gene expression. Mann-Whitney non-parametric test, *P< 0.05, n=5). (**D**) Model of Kiloscript and Hectoscript cells in the blastema during limb regeneration. Hectoscript cells express high levels of MKNK2 resulting in active suppression of translation. Inhibition of MKNK2 by cercosporamide releases this translational block enabling more Hectoscript cells to transit into Kiloscript cells, leading to proliferation and regeneration enhancement. Inhibition of MKNK2 may also affect other cells populations, thereby contributing additional boost to the noted enhancement of limb regeneration. MiR-10b present in the limb is downregulated after amputation in the local regenerating compartment. Downregulation results in local ribogene expression and increased protein synthesis. Conversely, a miR-10b synthetic mimic that substantially increases miR-10b, inhibits these events, thereby increasing the fraction of cells remaining in Hectoscript state. Consequently, fewer Kiloscript cells are generated leading to growth inhibition of the blastema.

Table S1. Morphology of the early limb regeneration in Cercosporamide-treated and control newts, Related to Figure 2. Larval *P. waltl* were treated with cercosporamide for 24h by immersion. The limb regenerates were evaluated 48 h after the treatment. Cercosporomide-1 µM, n = 12 (23x blastemas, 1x blastema was lost during processing); Control, DMSO n= 10 (20x blastemas). Cumulative data derived from two independent experiments. Note that limb blastema is an autonomous entity and respond differentially to the treatment from the same animals. e2D, early two-digit; FP, flat palette; LB, late blastema; MB, mid-blastema.

Treatment	**e2D**	**FP**	**LB**	**MB**
Cercosporamide (1 µM)	10 (43%)	03	09	01
Control (DMSO)	01 (5%)	04	13	02

Table S2. **Morphology of the limb regenerate in control and miR-10b mimic treated larval *P. waltl*, Related to Figure 4.** In all cases the right limb was injected with the mimic while the contralateral limb was served as the internal control. In all animals the limb amputation was performed at the mid humerus level. The mimic-injected limb regenerates showing delay to attain specific stages of regeneration are highlighted in yellow. Abbreviations: EB, early blastema; MB, mid blastema; LB, late blastema; P, Palette; 2D, two-digit stage; 3D, three-digit stage; 4D, four-digit stage, dpa, days post-amputation.

Animal #	Limb	10dpa	12dpa	14dpa	17dpa	20dpa	23dpa
1	Control	MB	LB	P	2D	3D	4D
	Mimic	EB	MB	LB	P	2D	4D
2	Control	LB	P	P	2D	3D	4D
	Mimic	MB	LB	LB	P	2D	4D
3	Control	EB	MB	LB	P	2D	3D
	Mimic	EB	EB	MB	LB	P	2D
4	Control	MB	LB	P	2D	4D	4D
	Mimic	EB	MB	LB	P	3D	4D
5	Control	LB	P	2D	2D	4D	4D
	Mimic	EB	MB	LB	P	2D	4D
6	Control	MB	LB	P	2D	3D	4D
	Mimic	MB	LB	LB	P	2D	4D
7	Control	LB	P	P	2D	3D	4D
	Mimic	MB	LB	P	P	2D	4D
8	Control	LB	P	P	2D	3D	4D
	Mimic	MB	LB	LB	P	2D	3D
9	Control	MB	LB	LB	P	2D	3D
	Mimic	MB	LB	LB	P	2D	3D

Table S3. List of primer sequences used for the detection of genes, Related to STAR Methods section.

MicroRNA name	**Primer sequence (5'-3')**
xtr-miR-10b-5p	UACCCUGUAGAACCGAAUUUGU
hsa-miR-222-3p	AGCUACAUCUGGCUACUGGGU
Gene name	**Primer sequence (5'-3')**
RPL4	F: CAACATGTGTCGTGGAGGTC R: TCTTCGATTCTGTGGCCCTT
RPL15	F: ACCAGATCAAGTTTGCCCGC R: GGTTGCGTCTGATAGCCTTG
RPL 27A	F: CAACCTGGATAAGCTCTGGAC R: ATCGATGATAGGGGCTGGTC
RPS 29	F: GTCATCAGCAGCTCTATTGGAG R: GCATACTGCCTGAAACACTGG
RPL30	F: TATCCTTGCCAACAACTGCC R: GGATCAATGATTGCCAATGTGC
GAPDH	F: ATCATTCCAGCCTCTACCGG R: CTGCTGCCTTTACCACCTTC